- Technical Paper -

MECHANISMS BEHIND DIMENSIONAL AND MASS CHANGES INDUCED BY ACCELERATED CARBONATION OF HARDENED CEMENTITIOUS MATERIALS

Karen Midori MASUNAGA[*1], Takeshi IYODA[*2]

ABSTRACT

Dimensional and mass changes induced by accelerated carbonation at 20% CO_2 were investigated in pre-conditioned OPC and GGBS blended cement hardened pastes. An abrupt mass increase followed by a slow ongoing mass decrease was observed, and the final mass change was positive for OPC, but negative for the blended pastes, which also exhibited larger shrinkage. The Calcium Carbonate filling effect is counteracted by the C-S-H decalcification shrinkage and the water release upon carbonation, the key mechanisms governing microstructural changes induced by accelerated carbonation.

Keywords: accelerated carbonation, carbonation shrinkage, C-S-H decalcification, GGBS.

1. INTRODUCTION

The carbonation mechanism of hydrated hardened cementitious materials was widely investigated in the past to understand and prevent its negative effects as a deterioration mechanism. While the natural carbonation phenomenon is a slow reaction, as the diffusion of CO_2 at low concentrations occurs at a rate of a few millimeters per year, in the accelerated carbonation the CO_2 concentration can be set up to 100% to achieve high CO_2 uptake in a short time and contribute to the Net Zero emissions in the cement and concrete industry. The carbonation technology proved to be more efficient when applied to hydrated cementitious materials than unhydrated cementitious compounds. However, if we consider that the carbonation reactions change the phase assemblage, it means that we are inducing the breakdown of the hydrated phases, as exemplified in Eq. 1 to Eq. 3, resulting in microstructural changes in the case of hardened materials. Despite the extensive range of reports about accelerated carbonation published in the last years, the efforts to quantify the CO_2 uptake have set aside some important phenomena related to the hydrated phases change, such as the C-S-H decalcification and the water release from the carbonation reactions, both of them resulting in dimensional and mass changes [1]. Therefore, in this study, the accelerated carbonation was investigated focusing on these two phenomena, in order to comprehend the mechanisms and the practical effects of mass and dimensional changes induced by accelerated carbonation in OPC and GGBS blended hardened pastes.

2. EXPERIMENTAL PROCEDURES

2.1 Materials and Methods

Considering the relevance of implementing supplementary cementitious materials and Carbon Capture Utilization and Storage (CCUS) admixtures, Ground Granulated Blast Furnace Slag (GGBS) and carbonated powder wastes from concrete recycling were used in the pastes' mixes. The description of the materials is shown in Table 1. The Calcium Carbonate (CC) content of the powder wastes was determined by thermogravimetric analyses (TGA) of the samples dried at 40°C to remove the adsorbed water, and the D50 was obtained from the particle size distribution measurement. The mix design is shown in Table 2. Pastes were mixed at high speed continuously for 3 minutes using a mortar mixer, and after they were mixed periodically until the bleeding was considered negligible. Specimens were cast, compacted using a vibration table, removed from the molds after 2 days of sealed curing, and then water cured until 91 days.

After the curing, specimens were pre-conditioned in a controlled chamber at 20°C, 60% relative humidity (RH) for 35 days, until when mass loss and drying shrinkage were considered stabilized. Then, specimens were placed inside a carbonation chamber 20% CO_2 concentration, 20ºC, 60% RH (CO_2 condition) with all surfaces exposed, without sealing. Parallelly, some specimens were kept in a chamber at 20°C, 60% RH with environmental CO_2 concentration (no CO_2 condition). The conditions are schematized in Fig. 1.

2.2 Experimental Tests

(1) Dimensional and mass changes

The dimensional change of (20x40x160)mm specimens with pins was measured using a digital length comparator instrument, with 0.001mm resolution, adapting the JIS A1129-3:2010. The average of three

Portlandite $Ca(OH)_2 + CO_2 \rightarrow CaCO_3 + H_2O$ (1)

C-S-H $(CaO)_x(SiO_2)_y(H_2O)_z + xCO_2 \rightarrow xCaCO_3 + ySiO_2 \cdot tH_2O + (z–t)H_2O$ (2)

Ettringite $3CaO \cdot Al_2O_3 \cdot 3CaSO_4 \cdot 32H_2O + 3CO_2 \rightarrow 3CaCO_3 + 3(CaSO_4 \cdot 2H_2O) + Al_2O_3 \cdot xH_2O + (26–x)H_2O$ (3)

*1 Graduate School of Engineering and Science, Shibaura Institute of Technology, M.E., JCI Student Member
*2 Professor, College of Engineering, Shibaura Institute of Technology, Dr.E., JCI Member

Table 1 Materials Description

Materials		Description	D50	CC content
OPC	Ordinary Portland Cement	Density = 3.14 g/cm^3; Blaine = 3530 cm^2/g; CaO = 65.01%.	-	4%
GGBS	Ground Granulated Blast Furnace Slag	Density = 2.91 g/cm^3; Blaine = 4030 cm^2/g; CaO = 40.00%.	-	-
LSP	Limestone Powder	Density = 2.77 g/cm^3; Blaine = 6800 cm^2/g; CaO = 55.51%.	6 µm	99%
RCAP	Recycled Concrete Aggregate Powder	Fine particles obtained from crushing and grinding of demolished concrete to produce recycled concrete aggregates.	46 µm	36%
CRCAP	Carbonated RCAP	Semi-wet carbonation of RCAP at CO_2 5%, 20°C, 60% RH for more than 14 days, keeping the water-solid ratio > 0.50.	39 µm	36%
CSW	Concrete Sludge Waste	Fine particles obtained from washing-out and filter-press of returned fresh concrete, after removing coarse and fine aggregates.	33 µm	7%
CCSW	Carbonated CSW	Semi-wet carbonation of CSW at CO_2 5%, 20°C, 60% RH for more than 14 days, keeping the water-solid ratio > 0.50.	15 µm	44%

Table 2 Pastes Mix Design

	Mix	Binder	Powder	Water/Binder (W/B)	Water/Powder (W/P)
1	N	OPC	-	0.60	-
2	B	B50 (50% OPC + 50% GGBS)	-		-
3	N-LSP	OPC	LSP		0.51
4	B-LSP	B50 (50% OPC + 50% GGBS)	LSP		0.51
5	N-RCAP	OPC	RCAP		0.51
6	B-RCAP	B50 (50% OPC + 50% GGBS)	RCAP		0.51
7	N-CRCAP	OPC	CRCAP		0.51
8	B-CRCAP	B50 (50% OPC + 50% GGBS)	CRCAP		0.51
9	N-CSW	OPC	CSW		0.51
10	B-CSW	B50 (50% OPC + 50% GGBS)	CSW		0.51
11	N-CCSW	OPC	CCSW		0.51
12	B-CCSW	B50 (50% OPC + 50% GGBS)	CCSW		0.51

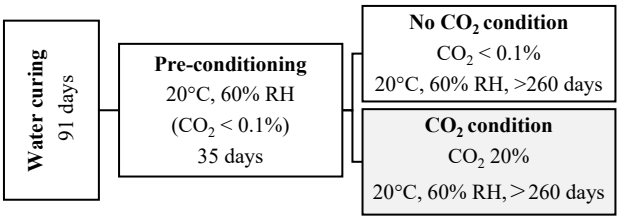

Fig. 1 Description of the experimental conditions.

measurements, using two specimens, was used in the calculations. The mass of these same specimens was recorded periodically using digital scales with 0.01g resolution, and the mass change ratio was calculated considering the mass after water curing as a reference.

(2) Flexural and compressive strength test

To investigate the accelerated carbonation effect on the mechanical properties, flexural and compressive strength were obtained according to the test procedures of JIS R5201:2015 (Physical Testing Methods for Cement), using (40x40x160)mm paste bars kept in CO_2 and no CO_2 conditions for more than 260 days.

(3) Porosity and capillary water absorption test

To evaluate the microstructural changes upon carbonation, the porosity of (40x40x80)mm paste specimens kept in CO_2 and in no CO_2 conditions for more than 260 days was determined. The porosity taking into consideration the presence of free water partially saturating the pores at 60% RH equilibrium was calculated, using the Archimedes method. For this, the mass just after carbonation/drying was recorded, then specimens were saturated in a vacuum chamber 0.1 MPa for 6 hours, and the saturated and submerged weight was measured. Then, the dry mass was obtained after drying at 40°C, 40% RH, until mass stabilization.

To evaluate the microstructural changes' practical effects on the mass transference properties, a simplified capillary water absorption test was applied to (40x40x80)mm specimens from the flexural test, without applying any drying process, to take into account the free water partially saturating the pores at 60% RH equilibrium. The non-fractured surface was positioned in 20 mm height of water and the mass of water absorbed by capillarity was recorded at 5, 10, 30, 60, 90, 150 minutes and 12 hours.

(4) Thermogravimetric analysis (TGA) test

TGA was conducted on a Netzsch STA25000, in an open vessel, using 25mg of hardened paste, cut just before the measurement in approximately 2mm cubic shape from the flexural test sample. The recordings were done continuously at a heating rate of 20°C/min, in N_2 atmosphere with flow rate of 150ml/min, at temperature range from 30°C to 1000°C, in 2 steps, keeping the sample at 40°C until mass stabilization, and then increasing the temperature until 1000°C. Differential thermal analysis (DTA), using Al_2O_3 as a reference sample, was also carried out to identify, for each sample individually, the initial and final temperatures of portlandite (CH) dehydroxylation (~470°C to 570°C) and CC decarbonation (~780°C to 900°C), and then to quantitatively determinate CH and CC contents, using the molecular masses of CH, H_2O, CC and CO_2.

In this study, the free water content of the samples was defined as the mass loss from the initial heating until 40°C, even though some mass decrease can be attributed to water loss from ettringite. The bond water was defined as the difference between the weight after 40°C drying and the weight at the temperature of CH dehydroxylation, identifiable in the non-carbonated samples, to separate it from the bond water in CH. For all quantifications, the initial mass was used as reference to intentionally include the free water in equilibrium at 60% RH after carbonation/drying in the discussions.

3. RESULTS AND DISCUSSIONS

3.1 Dimensional and Mass Changes

Initially, to simplify the results, the differences caused by the addition of the powder with CC will not be discussed, and we will focus only on the effects caused by the different cement types.

The Fig. 2 shows the dimensional change for OPC and B50 pastes. The negative days in the horizontal axis indicate the pre-conditioning period. For all samples, there was shrinkage, and in CO_2 condition (carbonation shrinkage) it was larger than in no CO_2 condition (drying shrinkage). Even though the drying shrinkage showed similar maximum values for different cements, the maximum carbonation shrinkage for the B50 ones was larger than the OPC, reaching nearly 1% for some B50 mixes. This indicated that the cement type significantly affects the extent of the dimensional change in CO_2 conditions and that carbonation shrinkage phenomenon is different than drying shrinkage.

The Fig. 3 shows the mass change for OPC and B50 pastes. After the initial mass loss during the preconditioning period, a rapid mass increase was observed for both cement type specimens in CO_2 conditions, reaching between 10-15% in a few days of carbonation. Comparing the initial inclination of the curve in CO_2 conditions, it is steeper for the B50 than the OPC pastes, indicating that the carbonation reactions and CC formation occurred more rapidly in the mixes with supplementary cementitious materials. The pre-conditioning removed partially the free capillary water, counterbalancing the water retention property of GGBS blended cementitious materials, and boosted the CO_2 diffusion which seems to have reached the full cross section of (20x40)mm in a few days, resulting in the rapid CC precipitation and mass increase. Another point

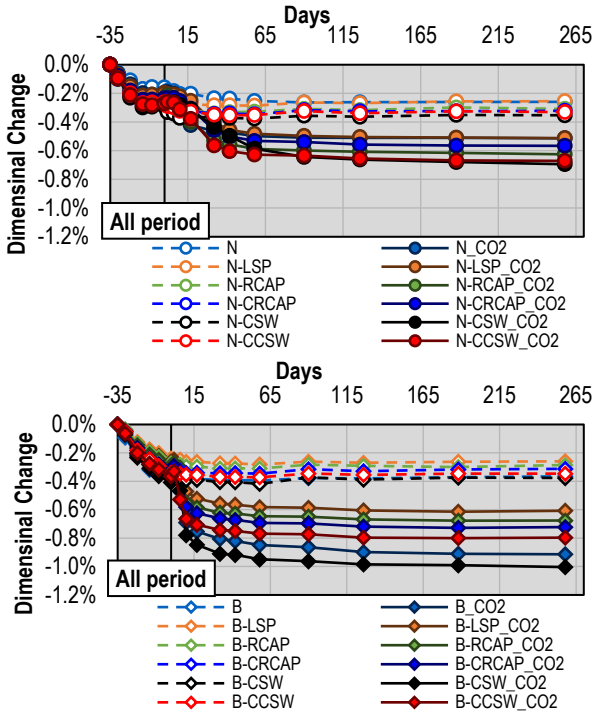

Fig. 2 Dimensional change of OPC pastes (above) and of B50 pastes (below).

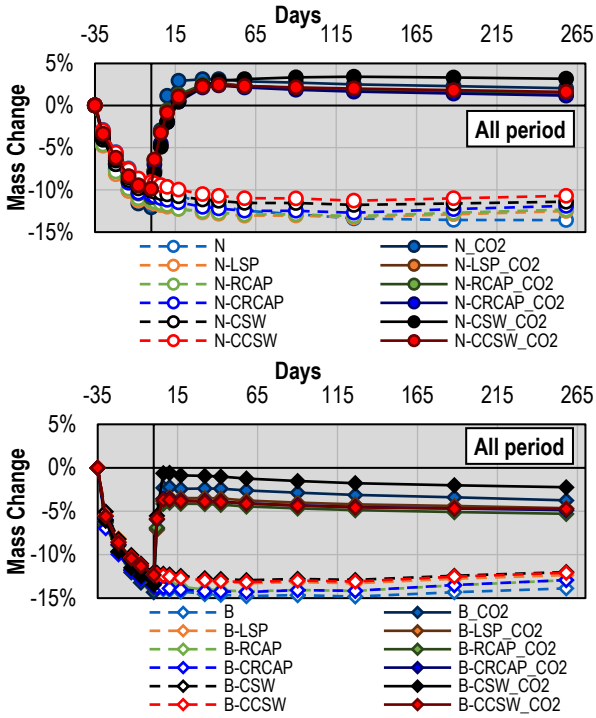

Fig. 3 Mass change of OPC pastes (above) and of B50 pastes (below).

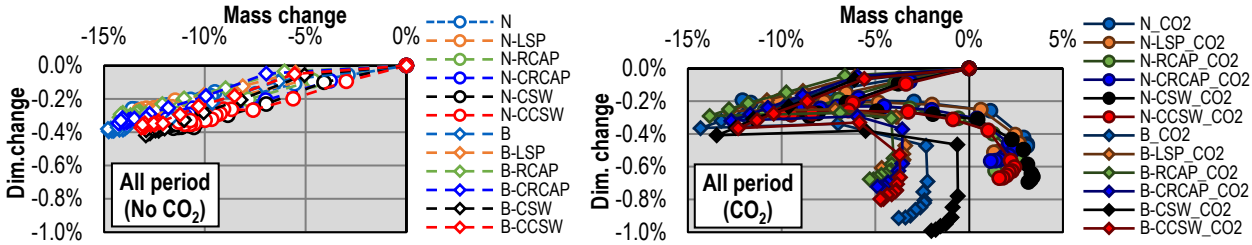

Fig. 4 Relationship between dimensional and mass changes for no CO_2 (left) and CO_2 condition (right).

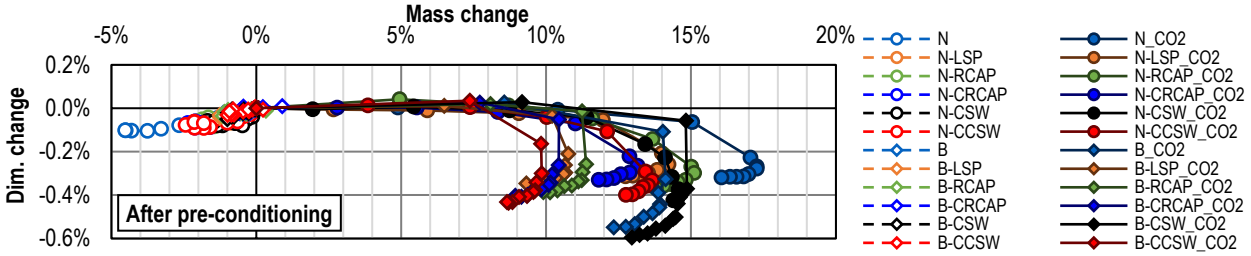

Fig. 5 Relationship between dimensional change and mass change, after pre-conditioning.

to be observed is that after the initial mass increase, there is a continuous and slow mass loss for all specimens, but more outstanding in the B50 pastes. As the specimens were pre-conditioned, the free capillary water had already evaporated until almost total equilibrium at 60% RH; therefore, this slight decrease in the mass suggests that after the carbonation reactions consumed the hydrates and precipitated CC, increasing the mass of the samples, H_2O was released from the hydrates, as shown in Eq. 1 to Eq. 3, and transformed into free water. The water released from carbonation reactions seems to be initially attached to the porosity but is slowly released in the 60% RH condition, which is not observed in the no CO_2 condition's specimens. Another hypothesis is that additional free water that was in equilibrium at 60% RH was released with porosity coarsening after carbonation. This will be discussed in the Section 3.3.

The relationship between dimensional change and mass change is shown in Fig. 4. For the no CO_2 condition, the drying shrinkage and mass loss continued to follow the linear trend of the pre-conditioning period, and it seems to have reached a stabilization, and there were no significant differences in the maximum shrinkage or mass change when comparing OPC and B50 pastes. This can be concluded from the agglomeration of the points for the no CO_2 condition, which occurred after the preconditioning. On the other hand, for the CO_2 condition, after the initial pre-conditioning in a linear trend, the pathway traced by carbonated OPC and B50 pastes was different than the no CO_2 condition and diverged. Even B50 showed a rapid mass increase, as discussed before, the OPC ones showed a larger mass increase, which can be explained by the higher CaO content reacting with CO_2, but the extent of the shrinkage was limited to less than 0.8%. This numerical number cannot be generalized as it relies on the specimens' shape and size, but when compared to the larger 1% shrinkage of some B50 specimens, it is possible to conclude that the phase assemblage of the pastes influences the dimensional and mass changes induced by accelerated carbonation. The measurements until 260 days seem to indicate that the length and mass changes reached relative convergence, sufficient enough to make consistent discussions and reliable conclusions, as seen from the horizontal trend lines in Fig. 2 and Fig. 3 and from the agglomeration of points in Fig. 4 for both no CO_2 and CO_2 conditions. However, measurements are being continued to verify if the convergence hypothesis is valid or if there will be some transition in the future.

The Fig. 5 shows the relationship between dimensional change and mass change, recalculated setting the initial reference as the measurement just before starting the carbonation, to exclude the influence of the pre-conditioning and evaluate only the dimensional and mass changes during the accelerated carbonation. This clarifies that, for the no CO_2 condition, some additional drying shrinkage and mass loss were observed. Therefore, it suggests that some mass loss and shrinkage from the drying of free water continued to occur together with carbonation. From here, the influence of adding powers containing CC will be discussed. After excluding the influence of the pre-conditioning, the trend followed by OPC and B50 specimens overlapped for some mixes. B and B-CSW followed a similar path of the OPC mixes, probably caused by the higher hydrates (non-carbonated CaO) content compared to the other B50 mixes, which contained already carbonated CaO (see Table 1). Also, in Fig. 5, when analyzing OPC and B50 pastes separately, the addition of the non-carbonated powder RCAP and the carbonated powders CRCAP and CCSW resulted in similar trends as adding pure limestone powder (LSP). The CC content of RCAP, CRCAP and CCSW is similar, which can explain similar dimensional and mass changes, considering that they may have similar microstructure and phase assemblage. However, the different particle sizes and the morphology of the CC may have influenced the progress of the carbonation front and the reactions, resulting in some discrepancies. Besides it, the filler and chemical effects of using CC from CCUS are a complex topic because of the additional influence of the fine particles from aggregate contamination. Regarding the similar result of LSP addition compared to the powders with lower CC content, it may indicate some saturation of the mix, and adding LSP, with 99% of a stable morphology CC (pure calcite), was not able to affect the microstructure and phase assemblage in a more positive way, resulting in similar results of dimensional and mass change when adding powders with around 40% of CC content.

In the case of OPC and B50 pastes evaluated in this study, the difference in the Ca/Si of C-S-H and in the CH content seem to be the main parameters influencing the dimensional and mass change in CO_2 conditions [1]. OPC usually contains C-S-H with Ca/Si ranging between 1.5 and 2.0, but SCM blended cements generally have lower Ca/Si (<1.6) due to the pozzolan reaction [2], which also consumes CH, reducing its content when a high degree of hydration is achieved. Also, from thermodynamic modeling prediction, the pH <10 after carbonation, measured by phenolphthalein spray, can be correlated to the reduction of Ca/Si until decalcification of C-S-H [3]. This scenario matches the experimental conditions of the pastes used in this study, cured for 91 days and carbonated for more than 260 days at high CO_2 concentration. Thus, the larger shrinkage in CO_2 condition for B50 compared to OPC suggests that the carbonation of initially low Ca/Si C-S-H may have occurred, leading to the phenomenon described as decalcification shrinkage of C-S-H. It was reported that pastes shrink significantly when the Ca/Si of C-S-H is reduced to values smaller than 1.2 [1]. As B50 samples were cured for more than 91 days, the pozzolan reaction consumed CH, producing C-S-H with lower Ca/Si than OPC [2]. Also, carbonation of CH tends to cause a volume expansion, whereas ettringite and C-S-H phases' carbonation led to the significant volume contraction [4]. Considering it, the lower initial Ca/Si ratio and the reduced CH content of B50 pastes than OPC may be associated with the larger shrinkage in CO_2 conditions.

In Fig. 4 and Fig. 5, it is also possible to see the slow ongoing mass decrease after the abrupt mass increase in the CO_2 condition, observed in the Fig. 3 along the time. This mass decrease occurs for both OPC

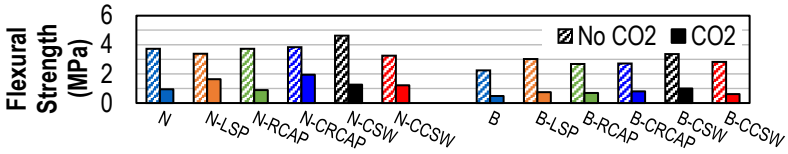

Fig. 6 Flexural strength of OPC and B50 pastes.

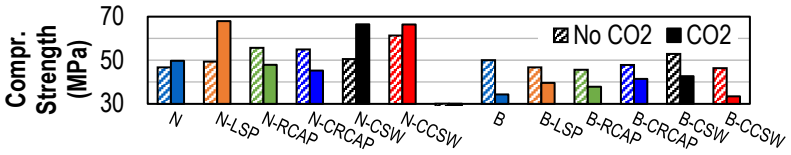

Fig. 7 Compressive strength of OPC and B50 pastes.

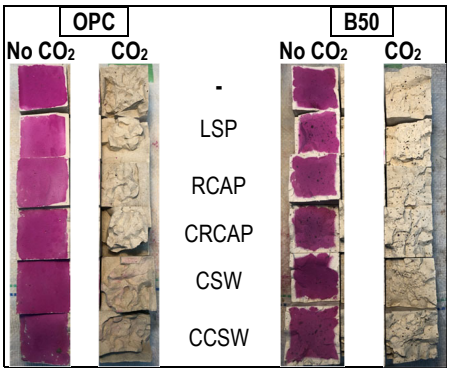

Fig. 8 Fracture pattern after flex. test.

and B50 pastes. But in the case of OPC, it is not followed by dimensional change, as occurs in the case of B50 pastes. Considering that the mass increase implies a high degree of carbonation and a large amount of CC precipitation inside the pores, in the case of OPC pastes, CC precipitation occurred from the carbonation of hydrates, such as CH and high Ca/Si C-S-H, refining the porosity. But for B50, the mass increase seems to come from the carbonation of low Ca/Si C-S-H, precipitating CC, similarly to OPC, but when Ca ions are removed from low Ca/Si C-S-H, the structures of C-S-H condense, leading to an increased shrinkage, porosity coarsening and release of water upon carbonation. Therefore, in the case of B50, some porosity coarsening and additional water evaporation explain the ongoing slow mass decrease and shrinkage, after the initial rapid mass increase and shrinkage. This will be discussed in the Section 3.3.

3.2 Flexural and Compressive Strength

Flexural and compressive strength for pastes in no CO_2 and CO_2 conditions are shown in Fig. 6 and Fig. 7. Considering the complexity of adding powders with different compositions and morphologies, each numerical value may not be easy to explain, but the tendency for OPC and B50 and the differences for no CO_2 and CO_2 conditions are compared in this section.

Flexural strength (Fig. 6), which is sensitive to the presence of microcracking, decreased significantly for all specimens kept in the CO_2 condition. From Fig. 8, it is possible to see a peculiar geometrical fracture pattern for both OPC and B50 carbonated specimens (non-colored, after phenolphthalein solution spray). This suggests that pre-existent microcracking from the carbonation shrinkage oriented the fracture in the bending test. The presence of cracks from carbonation shrinkage of the cement matrix was visible in the case of paste, but in mortar or concrete, where aggregates are present, the pastes' shrinkage may also make existent microcracking in the interfacial transition zone (ITZ) increase in length, width and number, diminishing the appearance of cracks in the paste specimens. Therefore, the same effect may not be visually identified but can result in a decrease of the mass transference properties and the mechanical properties, such as the Modulus of Elasticity. This needs to be investigated.

The compressive strength results (Fig. 7) confirm that CC precipitation in OPC specimens can strengthen the material. However, the influence of the microcracking seems also to have some effect, resulting in unpredictable results of decrease for some OPC mixes. In the case of B50 pastes, the microstructural changes from accelerated carbonation affected negatively not only flexural but also the compressive strength.

Summarizing, regardless of cement type, visible cracks from carbonation shrinkage were verified, as well as a decrease in the flexural strength of the carbonated specimens compared to the non-carbonated ones, as shown in the Fig. 6. The CC precipitation occurred for all OPC and B50 pastes, which was confirmed by TGA and X-Ray Diffraction (XRD), but the balance between the CC precipitation filling effect and the porosity coarsening from C-S-H decalcification shrinkage seems to be not the same depending on the cement type. The overall increase in the compressive strength for OPC indicates that CC filled the pores/cracks, increasing the bearing capacity, but the decrease for B50 suggests that some coarsening effect was more influential than this CC filling effect. Also, from the prolonged carbonation period and, thus, high carbonation degree, the presence of polymorphs of CC, with different molar ratios and characteristics, becomes significant [5]. Therefore, the differences in the formed polymorphs between OPC and B50 carbonated pastes might have some influence on the results and needs to be investigated.

3.3 Porosity and Capillary Water Absorption

The mass change from capillary water absorption of OPC and B50 pastes is shown in Fig. 9. The final mass increase of the carbonated specimens was smaller than the non-carbonated ones, but the saturation, especially of the B50 ones, was reached in a few minutes, contrasting with the non-carbonated ones, which continued to absorb water even after hours in contact with water. This occurred both for OPC and B50 pastes and seems to indicate a decrease in the water absorption potential of the carbonated specimens. However, if the specimens were larger, the mass change from water absorption might have continued to increase for the CO_2 specimens and exceed the total mass increase of the no CO_2 ones. This hypothesis of limitation in the specimens' size needs to be investigated. However, as samples were not dried before the test, the degree of saturation of carbonated and non-carbonated specimens was different, even at the same 60% RH. As seen in the volume composition (Fig. 10), calculated from the porosity test

results, CO_2 samples contained more free water partially saturating the pores (moisture) than the no CO_2 ones, at 60% RH equilibrium, and this can also be a reason why the total mass increase in the capillary absorption test was smaller for the CO_2 specimens. In addition, the microcracking from the carbonation shrinkage, discussed in the previous sections, may have interrupted the capillary pores and reduced the water absorption capacity. Comparing the differences in cement type, the saturation of the carbonated OPC specimens occurred between 6-8%, while for B50, it was between 8-11%. One probable reason is the porosity filling effect in carbonated OPC. From Fig. 10, all specimens in CO_2 condition showed reduced porosity (pores only, not considering the moisture) compared to no CO_2 condition, caused by the CC precipitation. However, after carbonation, the increase in moisture content of B50 samples is clearly higher than OPC samples. In other words, the filling effect of CC in B50 seems to have been counteracted by the porosity coarsening caused by low Ca/Si C-S-H decalcification, as discussed previously, and the water released from the hydrates' carbonation significantly influenced the microstructure and saturation of the pores, affecting the capillary water absorption capacity.

3.4 Phase Assemblage from TGA

A simplified phase assemblage, comparing the mass composition of pure OPC and B50 pastes in no CO_2 and CO_2 conditions, was calculated from TGA (Fig. 11). "Others" refers to the phase that is not free water, bond water, CH or CC, as defined in the Section 2.2(4). The reduced bond water content, the disappearance of CH and the CC formation in the carbonated samples confirmed the consumption of hydrates, such as C-S-H, ettringite and CH, to produce CC. The carbonation of crystalline phases was also verified by XRD (absence of ettringite and CH peaks and outstanding CC peaks). Also, in the no CO_2 conditions, both OPC and B50 contained more free water than in the CO_2 conditions, even at the same RH of 60%, confirming the occurrence of internal humidity change upon accelerated carbonation.

4. CONCLUSIONS

Dimensional and mass changes induced by accelerated carbonation were compared between OPC and 50% GGBS blended cement hardened pastes:

(1) The dimensional change induced by accelerated carbonation (carbonation shrinkage) seems to be a combination of decalcification shrinkage of C-S-H and additional drying shrinkage from the entrapped water and/or the water released from the carbonation reactions. Simultaneously, all pre-conditioned samples showed an initial rapid mass increase from CC precipitation, followed by a slow ongoing mass decrease, confirming the release of additional water and the occurrence of some internal humidity change upon accelerated carbonation. The shrinkage extent was larger for B50 than OPC, as well as the increase in moisture content with carbonation.

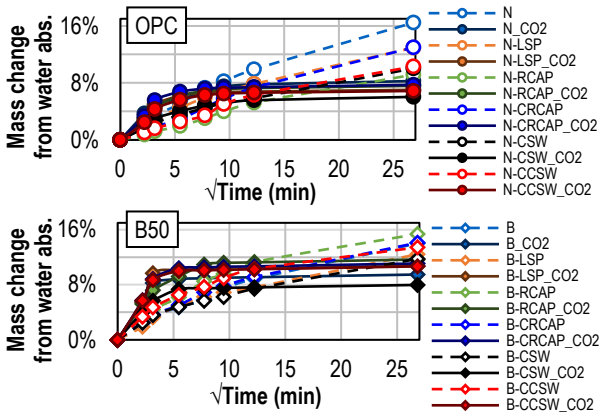

Fig. 9 Mass change from water absorption.

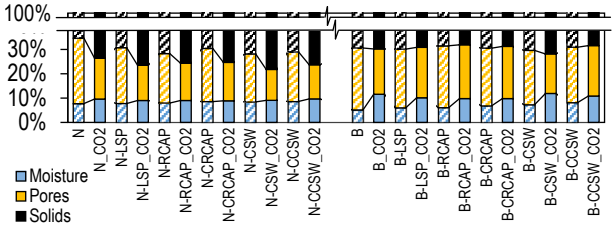

Fig. 10 Volume composition of OPC and B50.

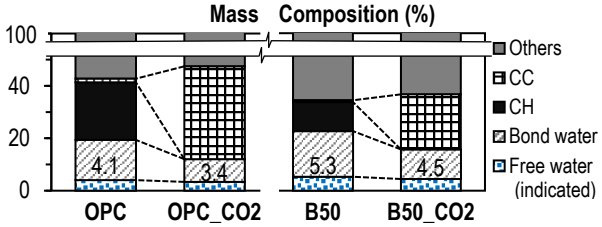

Fig. 11 Mass composition of OPC and B50.

(2) The microcracking from carbonation shrinkage reduced the flexural strength regardless of the binder. The balance between CC precipitation and C-S-H decalcification shrinkage resulted in overall increasing OPC's compressive strength, as CC filled the pores/cracks, reducing the porosity, but the decrease in B50's case was caused by a larger porosity coarsening than CC filling effect.

REFERENCES

[1] Chen, J.J. et al. "Decalcification shrinkage of cement paste," CCR 36, pp. 801-809, 2006.

[2] Lothenbach et al. "Supplementary cementitious materials," CCR 41, pp 1244-1256, 2011.

[3] Shi, Z. et al. Experimental studies and thermodynamic modeling of the carbonation of Portland cement, metakaolin and limestone mortars," CCR *88*, pp.60-72, 2016.

[4] Li, L. et al., "Dimensional change of cement paste subjected to carbonation in CO_2 sequestration and utilization context: A critical review on the mechanisms," Journal of CO_2 Utilization 70:102444, 2023.

[5] Morandeau et al. "Investigation of the carbonation mechanism of CH and C-S-H in terms of kinetics, microstructure changes and moisture properties," CCR 56, 153-170, 2014.